Design of superconducting magnetic energy storage (SMES) for waterborne applications

Carlos Hernando, Javier Munilla, Luis García-Tabarés, Carlos Gil, Nicolas Ballarín, Javier Orea, Rafael Iturbe, Borja López, Amalia Ballarino

***Abstract*— The shift from fossil fuel to electric based propulsion in the waterborne transport sector has been sped up by recent policies aiming to reduce the sector emissions. This trend creates highly electrified vessels, with needs for energy storage systems (ESS) to satisfy the power demand affordably and to increase the on-board grid reliability and efficiency. Initial industry efforts have been put in the study and integration of high energy density ESS solutions, mainly electrochemical batteries. However, other innovative ESS, with different capabilities, have not been yet fully addressed. It is the case of Fast Response Energy Storage Systems (FRESS), such as Supercapacitors, Flywheels, or Superconducting Magnetic Energy Storage (SMES) devices. The EU granted project, POwer StoragE IN D OceaN (POSEIDON) will undertake the necessary activities for the marinization of the three mentioned FRESS. This study presents the design process followed in the POSEIDON project for the definition of an SMES suitable for maritime operation. First, the boundary conditions imposed by the marine environment, and the potential on-board applications of the SMES will be established. Next, the technological options: superconducting material, cooling system, coil fabrication and magnet topology which have been selected for this specific system will be presented.**

***Index Terms*—** Superconducting magnetic energy storage, shipboard power systems, HTS coil.

I. INTRODUCTION

IN 2019, marine transportation accounted for approximately 4% of the total greenhouse gas (GHG) emissions within the European Union [1]. In order to meet the commitments, set forth by the COP21 Paris Climate Agreement, reducing GHG emissions has become a critical goal across all industrial sectors. To support this effort, the International Maritime Organization (IMO) has introduced comprehensive guidelines aimed at mitigating emissions of carbon dioxide (CO2), sulfur oxides (SOx), and nitrogen oxides (NOx) [2].

This work was supported by the European Union under grant agreement ID: 101096457. (*Corresponding author*: Carlos Hernando López de Toledo)

Carlos Hernando, and Carlos Gil are with CYCLOMED TECHNOLOGIES, Madrid, Spain and Carlos Hernando also with Comillas Pontifical University, Madrid, Spain (e-mail: c.hernando@cyclomed.tech).

Luis García-Tabarés, Javier Munilla, are with Centro de Investigaciones Energéticas, Medioambientales y Tecnológicas (CIEMAT), Madrid, Spain and Javier Munilla also with Comillas Pontifical University, Madrid, Spain.

Javier Orea and Nicolas Ballarin are with Comillas Pontifical University, Madrid, Spain.

Rafael Iturbe, and Borja Lopez, are with Antec Magnets SA.

Amalia Ballarino is with Centre Europeen de Recherche Nucleaire (CERN).

One common and effective way to follow these guidelines is by electrifying the propulsion system and other power needs on ships. The inclusion of energy storage systems (ESS) is essential for the substitution of combustion engines and the balancing of the power system [3].

Currently high energy density ESS, such as batteries or fuel cells are being considered for different maritime projects [4]. However, their relatively low power density, slow response, and restricted number of cycles limit their operation.

High power density ESSs have characteristics that could complement other ESSs, accelerating the electrical transition. In this paper, the marinization considerations and conceptual design of a superconducting magnetic energy storage system (SMES), that will be developed in the framework of an European project called POSEIDON [5] will be established.

II. ENERGY STORAGE APPLICATIONS ON-BOARD

Fast response ESSs (FRESS) are characterized by a number of advantages, particularly SMES offer: i) fast response; ii) high power density, iii) Unlimited number of charge/discharge cycles, iv) Uncritical deep discharge; v) Low toxicity. These characteristics provide higher quality to the power grid, and reduce the power limitations of high energy density ESS.

TABLE I.
SUMMARY TABLE OF TYPICAL VALUES FOR ESS TECHNOLOGY REQUIREMENTS, AND FRESS POTENTIAL INTEGRATION

Ship type	Discharge rate	Cycles	Energy Required	FRESS potential
Ferry	Very high	Very high	Average	High
OSV	Very high	Very low	Average	Medium
Cruise	Low	Likely high	Very high	Medium
Offshore drilling unit	Very high	Variable	Low	High
Fishing vessel	Average	Average	Average	Medium
Fish farm vessel	Average	Average	Average	Medium
Shuttle tanker	Very high	Very low	Average	Medium
Short sea shipping	Highly variable	Highly variable	Highly variable	Medium
Deep sea vessels	Highly variable	Highly variable	Highly variable	Medium
Bulk vessels with cranes	High	High	Low	High
Tug boats	Highly variable	Highly variable	High min. space)	Medium
Yachts	Low	Low	High	Low
High speed ferry	High	High	High	High
Wind farm support vessels	Very high	Very low	Average	Medium

With the data provide the EMSA [6] a classification of the most attractive type of vessels for FRESS integration have been established in TABLE I, where operational profiles with higher discharge rates and number of cycles are preferred.

Specific use cases for the identified target vessels have been already analyzed in the literature. The use of supercapacitors over Li-Ion batteries in a river ferry is studied in [7]. In [8] the addition of a FRESS to support the cranes of a bulk carrier vessel is analyzed. Both use cases showed a real potential for FRESS, however there has been limited FRESS integration in real world applications.

To overcome marinization and integration risks, EU-funded POSEIDON project have set two main technical goals: 1) To build 3 innovative marinized FRESS (SMES, Flywheel and Supercapacitors), with power capacities ranging 20-200 kW, and 2) To demonstrate 200 hours of operation in a maritime environment of a containerized system including the 3 developed FRESS systems.

Fig. 1 "Cap de Balearia" new BALEARIA electric ship, where POSEIDON project will test the developed energy storages systems.

III. POSEIDON SMES

A. Marinization and design guidelines

The development of a SMES system is mainly focused on two tasks, superconducting magnet design including cooling system, and the power conditioning system (PCS), which is the interface between the magnet and the power grid.

Typically, the main constraints imposed on a SMES come from the application, i.e. the required energy and power, the DC link voltage, and the dynamic response. However, there are additional constraints for its use in waterborne applications. TABLE II provides a summary of these constraints and the limit values established for compliance in the POSEIDON project based on existing regulations for ESS, and electrical machines in vessels [9]–[13], and the use of the high magnetic field equipment near people [14].

TABLE II.
MARINIZATION CONSTRAINTS OF POSEIDON SMES

Electromagnetic	Magnetic Field	0.5 mT @ 0.5 m. from cryostat wall
Mechanical	Acceleration	– Heave 0.4 g – Surge 0.25 g
	Vibrations	– Mode 1: 2,0 Hz to 13,2 Hz: displacement amplitude of 1,0 mm – Mode 2: 13,2 Hz to 100 Hz: Acceleration amplitude of 0,7 g
Physical	Ambient temperature, humidity and salinity	$0 \leq T_{SMES,t} \leq 45ºC$ $25\% \leq RH \leq 100\%$

These constraints have been included in the optimization process of the SMES, and although most are mitigated at the container level, certain aspects, like the vessel angular accelerations must be taken into account during the magnet mechanical analysis.

The final design incorporates a high-temperature superconducting (HTS) magnet constructed from a stack of insulated double-pancake coils. HTS was chosen over other superconducting materials [15] due to its compatibility with simplified and safer cryogenic systems, as well as its potential for long-term cost competitiveness in light of current market trends. Insulation is required to enable the magnet to operate at high voltages and achieve high power densities. TABLE III summarizes the key parameters of the magnet and coil. The following sections will provide a detailed analysis of the magnet design.

TABLE III.
MAIN PARAMETERS OF THE POSEIDON SMES

	Parameter	Value
SC material	Material	2G HTS Tape
	Supplier	Shanghai Superconductors
	Dimensions	4.8 mm width & 0.34 mm (Cu lamination & Kapton insulation, see TABLE IV)
SC coil	Internal radius	86 mm
	Cross section	49x10 mm^2
	Turns	144 per coil (200 m. of tape)
Magnet	Nº of Double pancakes	12
	Topology	Solenoidal
	Inductance	1.68 H
	Nominal current	457A @4.2K (220A @20K) (80% of critical current)
Cooling system	Operating temperature	4.2K@LHe bath (20K in operation)
Power and control system	Topology	Voltage Source Converter
	Voltage	500-600 V
SMES	Energy	275 kJ (@ 4.2K)

B. Electromagnetic Design

The selection of the final geometry obeys to the maximization of the specific energy per meter of superconducting tape, which typically derives coils with big bores. However, for the POSEIDON SMES, the maximum dimensions of the SMES were limited due to the final application physical limitations. Therefore, the coil size was predefined, and its dimensions are given in TABLE II, which left the pancakes separation distance as the only variable for optimization.

Two models have been developed for electromagnetic optimization, both employing a 2D axisymmetric approach to simulate time-dependent electromagnetic behavior. The first model is an in-house tool developed in MATLAB, utilizing the A-ϕ integral formulation [16]. The second model is implemented in COMSOL, based on the H-formulation.

The MATLAB model is utilized for the optimization process due to its significantly lower computational time, while the COMSOL model is employed for verification.

Both models account for self-field effects, as well as the magnetic field magnitude and angle-dependent current density distribution. A fitted function for the critical current Ic (B,θ) [17], which coefficients have been adapted to fit supplier data, has been employed, along with a non-uniform current density distribution.

A typical current profile in a SMES system follows a trapezoidal shape, characterized by a slow charging phase (although it can be high to accommodate sudden changes in power), a plateau at the nominal current, and a rapid discharge when power is required. For this electromagnetic analysis, a worst-case scenario is considered, where each phase lasts 1 second. Fig. 2 depicts the normalized current density (J/J_c) distribution of the magnet at two moments: fully charged (left) and discharged (right). When the coil is discharged, negative current densities start to appear in the tape borders, and penetrate to the interior compensating existing positive current densities. This effect creates persistent screening currents even when the coil is discharged. However, the simulation may overestimate this effect, due to the axisymmetric assumption and the non-inclusion of the resistive joints.

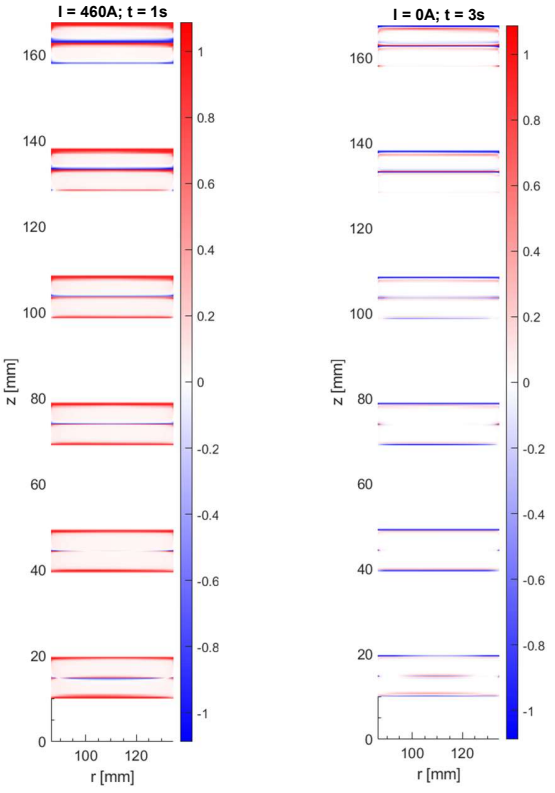

Fig. 2 Normalized current density $\left(\frac{J}{Jc}\right)$ distribution of the POSEIDON magnet assembly. Only the upper half of the magnet coils are depicted, where z = 0 mm represents the midplane.

Once the distributions of the magnetic field and current density are worked out from the electromagnetic model, the Lorentz forces are computed, which are exported to the mechanical model.

C. *Mechanical design*

A bulk model approach has been utilized in which the coil cross section has been approximated by an equivalent homogenous material made of a stack of REBCO tapes and resin. The homogenization has been done with the material modeler module in Ansys.

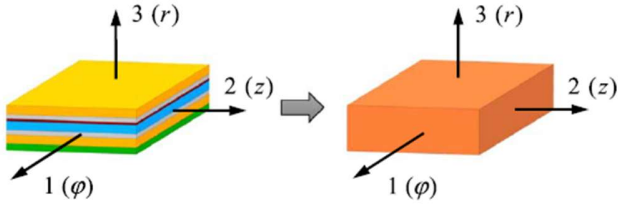

Fig. 3. Equivalent homogeneous material for the wet wound insulated REBCO tape.

The constituent material properties are given in TABLE IV [5], [6], as well as the equivalent homogenized coil properties, and the G10 former employed for winding and mechanical support. Properties have been validated experimentally.

TABLE IV.
MECHANICAL PROPERTIES OF MAGNET MATERIALS AT WORKING TEMPERATURE

Component	Thickness (mm)	E_m (GPa)	ν_m	G_m (GPa)	$\Delta L/L$ (@296-4.2K)
Copper	170	138	0.34	52	2.9e-3
Ag+Buffer	4	90	0.3	35	4.1e-3
REBCO	1.6	125	0.34	69	-
Hastelloy C-276	50	210	0.3	81	3.1e-3
Kapton	100	2.5	0.35	0.93	1.0e-2
Resin	2	7	0.28	2.75	6.4e-3
Homogenized coil material					
HTS φ (φz)	--	98.9	0.32	39.8	3.4e-3
HTS z (zr)	--	98.9	0.016	4.49	3.4e-3
HTS r ($r\varphi$)	--	6.15	0.016	4.49	4.6e-3
G10 Mandrel					
G10 φ (φz)	--	30	0.33	10	2.4e-3
G10 z (zr)	--	30	0.33	5	2.4e-3
G10 r ($r\varphi$)	--	9	0.2	5	7.1e-3

A 2D axisymmetric mechanical analysis is performed in Ansys to estimate the magnet stresses. The main boundary condition considered is the no vertical displacement in the upper and lower plates of each coil.

The analysis was performed in three steps. First, the stress and strain induced by the thermal contraction from the cooling to 4.2K is evaluated. Second, the force obtained from the worst case of the electromagnetic design, i.e the magnet operating at 4.2K and at nominal current is transferred from the electromagnetic model to the mechanical interface.

Fig. 4 illustrates the maximum hoop and radial stresses for each coil. Due to symmetry, only half of the coils are depicted, with coil 1 being closest to the magnet midplane. Coil 2 exhibits the highest stress values, with maximum hoop and radial stresses reaching 198 MPa and 15 MPa, respectively.

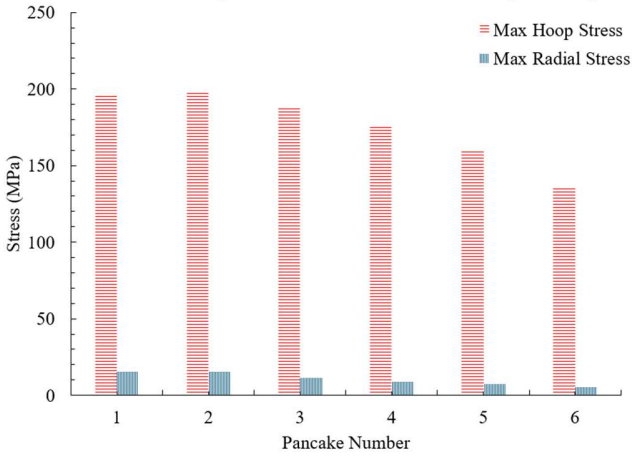

Fig. 4. Maximum hoop and radial stress for each pancake

Fig. 5 shows the hoop and radial stress distribution for the most stressed coil, pancake 2. In this figure the G10 former is suppressed to improve visual clarity.

The elastic limit of the tape is not surpassed, and the radial stresses are mostly negative, however positive stresses are observed in the upper side of the inner section of the coil due to the distribution of the Lorentz forces. The possibility of increasing the winding tension, which has not been included in the analysis, will be studied to failure risk.

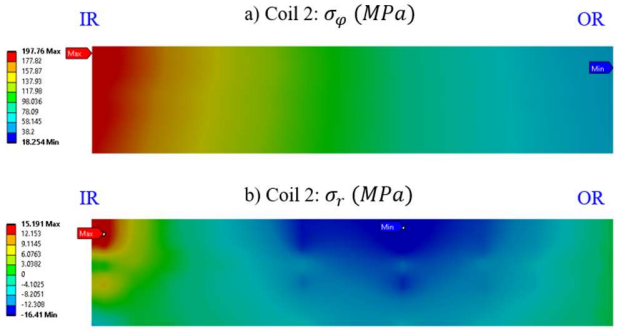

Fig. 5. Distributions of (a) hoop stress and (b) radial stress in coil 2 based on the bulk model.

D. *Cooling system*

The initial magnet tests will be conducted in laboratory facilities using a liquid helium (LHe) bath. However, the cooling system for the final application will utilize flow refrigeration, which cools via forced convection of gaseous helium. This method provides an autonomous, cost-effective, and compact solution capable of localized heat rejection, with the flexibility to operate across a temperature range of 4.2 K to 77 K. A system based on this design, known as the Cryogenic Supply System (CSS), has already been successfully tested in other superconducting applications [18].

The optimization of the cooling system will be guided by the test campaign results and the validation of the electromagnetic model. This will ensure accurate computation of AC losses, which are anticipated to be the primary thermal load on the system.

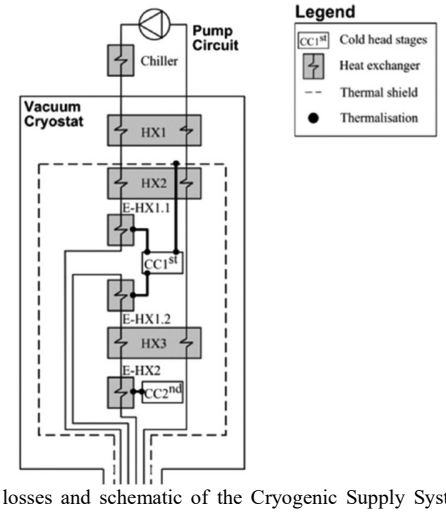

Fig. 6, Thermal losses and schematic of the Cryogenic Supply System (CSS)

E. *Power and control system (PCS)*

The selected PCS is a voltage source converter formed by a grid side inverter based on IGBTs and a dc-dc chopper.

The control strategy is based on keeping a constant voltage across the dc-link capacitor. This option allows the exchange of power in the four quadrants as can be selected from zero to 360º. This solution is characterized by an intermediate value of Total Harmonic Distortion (THD) and also a medium ripple in the voltage applied to the coil leading to moderate losses.

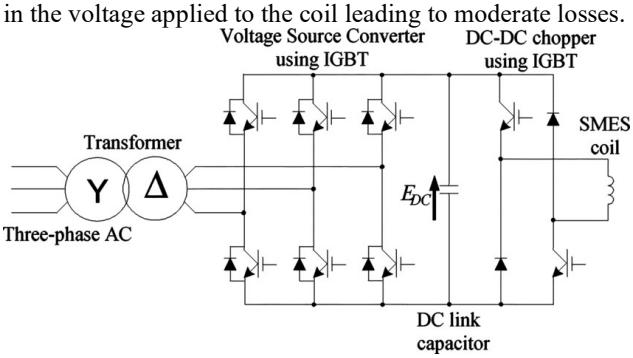

Fig. 7 Voltage Source Converter PCS schematic

V. Conclusion

Several vessels in the waterborne sector have been identified as candidates for the integration of a FRESS system to accelerate the energy transition. To mitigate technical and integration risks, the POSEIDON project will develop and marinize a HTS SMES for use in an electric ferry.

Marinization constraints, aligned with existing regulations, have been defined and used to establish the initial design parameters of the SMES. A comprehensive electromagnetic and mechanical analysis of the magnet has been completed. The manufacturing and validation phase of the system is now underway, during which testing protocols will be developed and implemented to validate the marinization of the SMES. These constraints will be refined based on insights gained during the project.

REFERENCES

[1] "Emissions from planes and ships: facts and figures (infographic) | News | European Parliament." Accessed: Sep. 25, 2023. [Online]. Available: https://www.europarl.europa.eu/news/en/headlines/society/20191129STO67756/emissions-from-planes-and-ships-facts-and-figures-infographic

[2] International Maritime Organization, "International Maritime Organization: Prevention of Air Pollution from Ships." [Online]. Available: https://www.imo.org/en/OurWork/Environment/Pages/Air-Pollution.aspx

[3] M. U. Mutarraf, Y. Terriche, K. A. K. Niazi, J. C. Vasquez, and J. M. Guerrero, "Energy Storage Systems for Shipboard Microgrids—A Review," *Energies 2018, Vol. 11, Page 3492*, vol. 11, no. 12, p. 3492, Dec. 2018, doi: 10.3390/EN11123492.

[4] S. Jafarzadeh and I. Schjølberg, "Emission Reduction in Shipping Using Hydrogen and Fuel Cells," *Proc. Int. Conf. Offshore Mech. Arct. Eng. - OMAE*, vol. 10, Sep. 2017, doi: 10.1115/OMAE2017-61401.

[5] "POwer StoragE In D OceaN | POSEIDON | Project | Fact sheet | HORIZON | CORDIS | European Commission." Accessed: Sep. 25, 2023. [Online]. Available: https://cordis.europa.eu/project/id/101096457

[6] EMSA European Maritime Safety Agency, "STUDY ON ELECTRICAL ENERGY STORAGE FOR SHIPS," 2019.

[7] N. Bennabi, H. Menana, J. F. Charpentier, J. Y. Billard, and B. Nottelet, "Design and Comparative Study of Hybrid Propulsions for a River Ferry Operating on Short Cycles with High Power Demands," *J. Mar. Sci. Eng. 2021, Vol. 9, Page 631*, vol. 9, no. 6, p. 631, Jun. 2021, doi: 10.3390/JMSE9060631.

[8] K. Kim, J. An, K. Park, G. Roh, and K. Chun, "Analysis of a Supercapacitor/Battery Hybrid Power System for a Bulk Carrier," *Appl. Sci. 2019, Vol. 9, Page 1547*, vol. 9, no. 8, p. 1547, Apr. 2019, doi: 10.3390/APP9081547.

[9] American Bureau of Shipping, "USE OF SUPERCAPACITORS IN THE MARINE AND OFFSHORE INDUSTRIES," 2017.

[10] N. Mjøs *et al.*, "DNV GL Guideline for large maritime battery systems," 2014. Accessed: Jun. 12, 2023. [Online]. Available: www.dnvgl.com

[11] Narve Mjøs, Sverre Eriksen, Andreas Kristoffersen, Gerd Petra Haugom, and Asmund Huser, "DNV GL Handbook for Maritime and Offshore Battery Systems," 2016. Accessed: Jun. 12, 2023. [Online]. Available: www.dnvgl.com

[12] U. C. of E. on the T. of D. Goods and U. E. Secretariat, "Recommendations on the transport of dangerous goods.: Model Regulations.: Volume 1," *Recomm. Transp. Danger. goods - Model Regul.*, vol. Volume I, pp. 49–181, 2019, Accessed: Jun. 12, 2023. [Online]. Available: https://digitallibrary.un.org/record/3830095

[13] "Deliverables - Current Direct." Accessed: Jun. 12, 2023. [Online]. Available: https://www.currentdirect.eu/deliverables/

[14] Official Journal of the European Union, *DIRECTIVE 2013/35/EU OF THE EUROPEAN PARLIAMENT AND OF THE COUNCIL*. 2013.

[15] C. Hernando, J. Munilla, L. Garcia-Tabares, and G. Pedraz, "Optimization of High Power SMES for Naval Applications," *IEEE Trans. Appl. Supercond.*, vol. 33, no. 5, Aug. 2023, doi: 10.1109/TASC.2023.3250169.

[16] S. Otten and F. Grilli, "Simple and Fast Method for Computing Induced Currents in Superconductors Using Freely Available Solvers for Ordinary Differential Equations," *IEEE Trans. Appl. Supercond.*, vol. 29, no. 8, Dec. 2019, doi: 10.1109/TASC.2019.2949240.

[17] H. Maeda and Y. Yanagisawa, "Recent Developments in High-Temperature Superconducting Magnet Technology (Review)," *IEEE Trans. Appl. Supercond.*, vol. 24, no. 3, Jun. 2014, doi: 10.1109/TASC.2013.2287707.

[18] J. Munilla *et al.*, "Commissioning of an Autonomous Cooling System for a Compact Superconducting Cyclotron Devoted to Radioisotope Production," *IEEE Trans. Appl. Supercond.*, vol. 31, no. 5, Aug. 2021, doi: 10.1109/TASC.2021.3070118.